Dispersion of Viscous Liquids by Turbulent Flow in a Static Mixer

Drops are stabilized in agitated liquid-liquid systems by both surface and internal viscous forces. The dispersion of an inviscid liquid into a turbulent continuous phase in static mixers has been studied but the effect of dispersed phase viscosity is not well understood. Systematic experiments have been conducted in a Kenics mixer by photographically examining dilute suspensions of viscous oils in water to determine how viscosity and conditions of agitation affect equilibrium mean drop size and size distribution. A semiempirical theory is developed which correlates the mean size data and collapses to the well-known Weber number result in the inviscid limit. A correlation for drop size distribution in terms of cumulative volume frequency is developed by normalization with the Sauter mean diameter D_{32}. Measurements at the mixer entrance indicate that the method of introduction of the dispersed phase should be considered when evaluating mixer performance.

Paul D. Berkman, Richard V. Calabrese
Department of Chemical and Nuclear Engineering
University of Maryland
College Park, MD 20742

Introduction

While the determination of interfacial area for liquid-liquid dispersions produced in turbulent stirred-tank contactors has commanded considerable attention (Tavlarides and Stamatoudis, 1981), few studies have focused upon continuous, in-line mixers. Yet static mixers offer an attractive alternative to stirred vessels due to narrower residence time distribution, lower capital and operating costs, and minimal maintenance requirements.

Middleman (1974) measured drop size distributions in Kenics mixers by producing dilute suspensions of six different organic liquids in water. He found that equilibrium was achieved after about $n_e = 10$ mixer elements. For inviscid dispersed phases ($\mu_d \leq 1$ mPa · s) the equilibrium data were well correlated by

$$\frac{D_{32}}{D_o} = AWe^{-3/5} \tag{1}$$

where $We = \rho_c \bar{V}^2 D_o/\sigma$ is the system Weber number. Middleman derived Eq. 1 by assuming that the disruptive energy acting upon a drop was due to inertial subrange eddies and that drop stability was due only to interfacial tension. A slight dependency on Reynolds number resulted and was ignored. As expected, Eq. 1 failed to correlate his data for $5 \leq \mu_d \leq 26$ mPa · s. Equilibrium drop size distributions were found to be normally distributed in volume and were correlated by normalization with the Sauter mean diameter D_{32}. Additional data for benzene-water dispersions ($\mu_d = 0.6$ mPa · s) showed that mean drop diameter was independent of dispersed phase volume fraction for $0.01 < \Phi < 0.25$.

Chen and Libby (1978) dispersed kerosene and mineral oil in water in a Kenics mixer. They correlated mean drop size data, empirically, in terms of Weber number and viscosity ratio. A single drop size distribution was reported. Al Taweel and Walker (1983) measured mean drop size for dilute dispersions of kerosene in water in two different configurations of a Lightnin "In-liner" mixer. The systematically varied energy dissipation rate (average velocity) and the number of mixer elements (residence time). They reported the number of elements required to achieve equilibrium and found that their data could be correlated in terms of energy dissipation rate or Weber number. A quantitative measure of dispersion efficiency was also given. Recently, Haas (1987) has evaluated several devices for the production of nuclear fuels via the gel sphere process. Kenics mixer data for the dispersion of water into organics were correlated empirically in terms of Weber number, Reynolds number, and viscosity ratio.

This study extends previous work by examining the extent to which internal viscous resistance to breakage affects equilib-

Correspondence concerning this paper should be addressed to R. V. Calabrese.
P. D. Berkman is presently with Naval Ordnance Station, Indian Head, MD.

rium mean drop size and drop size distribution for turbulent flow through a static mixer. Mixer performance is evaluated from photographic observations of drop size at the entrance and exit of a 24-element Kenics mixer. Systematic experiments for dilute suspensions of various oils ($0.63 \leq \mu_d \leq 204$ mPa · s) in water indicate that equilibrium mean drop size increases and the size distribution broadens with increasing dispersed phase viscosity and decreasing Reynolds number (or energy dissipation rate).

Equation 1 is extended via mechanistic arguments to include the effect of dispersed phase viscosity. Mean drop size is shown to depend on two system parameters: the Weber number *We*, and a viscosity group *Vi* representing the ratio of dispersed phase viscous to surface forces. The two geometric constants in the resulting semiempirical equation are obtained from linear regression of the data. In the inviscid limit this correlation provides an equally good fit to the low-viscosity dispersed phase data of Middleman (1974).

Equilibrium drop sizes are found to be normally distributed in volume. A correlation that applies to both inviscid and viscous dispersed phases is developed via nonlinear least-squares regression by normalization of the cumulative volume frequency data with D_{32}. A comparison of size distributions at the entrance and exit of the mixer indicates that the method of introduction of the dispersed phase should be considered when evaluating mixer performance.

The effect of system variables on and the form of the correlations for equilibrium mean drop size and size distribution are found to be the same as for turbulent stirred-tank contactors.

Experimental Method

The 24-element, 1.91 cm dia. stainless steel Kenics mixer has a pitch (L_e/D_o) of 1.5. Middleman's (1974) data indicate that 10 elements are sufficient to achieve equilibrium. This longer mixer was selected since more viscous dispersed phases are employed here, and it is prudent to assume that the effect of μ_d is to increase the time (distance) to reach equilibrium.

A diagram of the experimental facility is given in Figure 1. Filtered tap water is fed from a 120 L constant-head tank through 15.2 cm dia. PVC pipe to a point below the test section. It then passes through a U bend and reducer so that it becomes directed vertically upward through a 1.91 cm ID clear acrylic tube. The bell-shaped reducer is designed to minimize flow disturbances. The test section is located in the acrylic tube with the mixer entrance at 50 tube diameters downstream from the reducer. The flow exiting the mixer passes through a metering valve and a flexible hose and then into a collecting tank for discharge to a drain. The volumetric flow rate was obtained by moving the discharge of the flexible hose to a large glass cylinder and measuring the time to collect 20 L of water. The pressure drop across the mixer was measured with static head tubes connected to pressure taps in the test section wall.

Since building water was used, it was difficult to control temperature. However, water and room temperature did not differ substantially and remained constant during any given run. A seasonal temperature variation of several degrees was accepted to avoid complications associated with recirculation and removal of the dispersed phase from a more controllable closed-loop system.

The dispersed phase was introduced through a 0.25 cm ID, 0.32 cm OD, stainless steel capillary tube which passes through

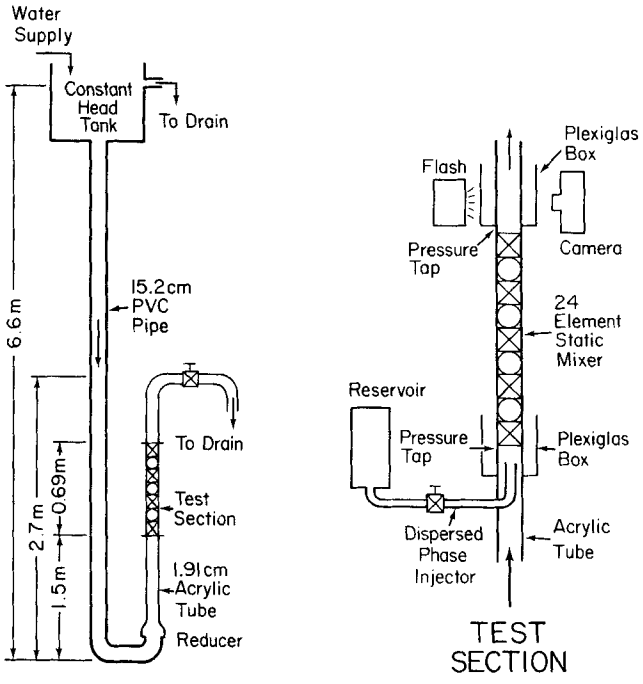

Figure 1. Experimental facility

the acrylic tube wall and makes a 90° turn so that its vertical leg is concentric with the axis of the acrylic tube. The vertical leg is 15 capillary tube diameters long with its exit located about 9 cm below the mixer entrance to insure that drops produced by it relax to a spherical shape before entering the mixer. The injector tube is fed by gas pressure from a 1.5 L stainless steel reservoir. The flow rate is regulated by a calibrated metering valve.

Small square, water-filled Plexiglas boxes surrounding the test section were used to eliminate optical distortion while photographing the dispersion. The initial drop size distribution was acquired just below the mixer entrance. The final distribution was measured about 10 cm above the mixer exit to allow exiting oil globules to relax to a spherical shape. Photographs were taken with a Nikon F3 35 mm SLR camera equipped with an MD-4 motor drive, a PB-6 bellows, and a reverse-mounted 55 mm Micro-Nikor lens. Magnifications from 1.5 to 3 times actual size were achieved. This configuration provided small depth of field and negligible parallax error. Illumination was provided by a Sunpak 611 automatic thyristor flash unit placed opposite the camera. The flash duration of 1/30,000 s was sufficiently fast to freeze droplet motion.

Drop sizes were measured from the negatives (Kodak Technical Pan Film 2415) and the data were analyzed to obtain Sauter mean diameter and cumulative volume frequency as described by Wang and Calabrese (1986). Initial and final drop size distributions were determined from at least 100 and 300 counts of drop size, respectively.

Seven different dispersed phase fluids were employed. Physical properties are given in Table 1 at the temperatures of the experiments. Each oil is assigned a nominal viscosity μ_d' to facilitate subsequent discussion. Viscosity, density, and interfacial tension with filtered tap water were measured as in Wang and Calabrese (1986). Handbook data were used for the density and viscosity of water. Table 1 shows that a wide range of dispersed phase viscosity was considered. The range of interfacial tension

Table 1. Physical Properties of Dispersed Phases

Dispersed Phase	Nominal Viscosity μ_d' mPa · s	Temp. °C	Viscosity μ_d mPa · s	Density ρ_d g · cm^{-3}	Interfacial* Tension σ mN · m^{-1}
Silicone oil	20	21	19.6	0.947	37.4
	20	22	19.4	0.946	37.4
	50	20	51.8	0.963	37.4
	50	22	49.9	0.961	37.4
	50	23	49.0	0.960	37.4
	100	22	103	0.962	37.4
	200	21	204	0.967	37.4
	200	22	201	0.966	37.4
Paraffin oil	45	23	46.1	0.853	41.6
	45	24	43.0	0.852	41.6
	150	23	161	0.876	41.6
	150	24	151	0.875	41.6
	150	25	141	0.874	41.6
p-Xylene	0.6	21	0.64	0.857	31.8
	0.6	22	0.63	0.856	31.8

*With water (continuous phase).

was limited since its role has been systematically studied by Middleman (1974).

For each dispersed phase, experiments were conducted at pipe Reynolds numbers Re of 12,000, 15,000, 18,000, and 21,000. $Re = \bar{V}D_o/\nu_c$ is based upon the average velocity of the continuous phase ($0.58 < \bar{V} < 1.05$ m/s) since Φ was too small to affect total flow rate.

The constraints placed upon the oil injector were to produce large drops of narrow size distribution at a dispersed phase holdup of less than 0.1% by volume. This proved to be difficult. The injector flow may be viewed as a capillary jet discharging into a coflowing turbulent stream, a system for which design data are lacking. Initial experiments with different capillary tubes revealed that the action of the surrounding turbulence dictated the use of the selected injector at minimum discharge velocity. For each run the injector flow rate was adjusted while visually observing the capillary jet with a strobe light to achieve an acceptable result. Therefore, actual holdups were in the range $0.00057 \leq \Phi \leq 0.001$. Nevertheless, it was necessary to accept the presence of some small satellite droplets, particularly for the more viscous oils, and to account for their presence in evaluating mixer performance.

Detailed data for each run are given by Berkman (1985).

Results

The pressure drop measurements were converted to Fanning friction factors (Bird et al., 1960) by:

$$\Delta P = \frac{4L}{D_o}\frac{1}{2}\rho_c \bar{V}^2 f \tag{1}$$

The results, given in Figure 2, show that the friction factor is constant ($f = 0.416$) for $Re \geq 12{,}000$ and is about 50 times greater than those for a smooth pipe. Middleman (1974) assumed that f showed a dependency on Re similar to that for a smooth pipe. These data show a stronger analogy to a rough pipe. Mean energy dissipation rates may be estimated from:

$$\bar{\epsilon} = \frac{\bar{V}\Delta P}{\rho_c L} \tag{2}$$

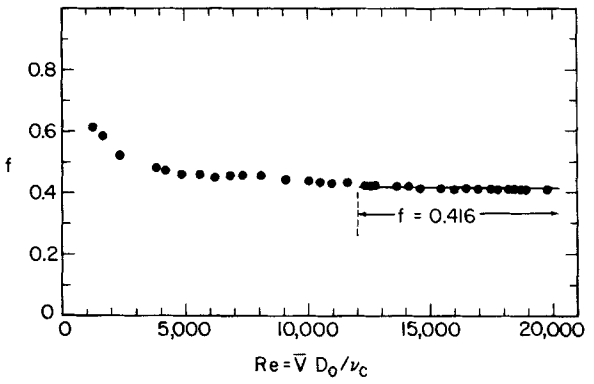

Figure 2. Fanning friction factor for Kenics static mixer.
$n_e = 24$; $D_o = 1.91$ cm; $L_e/D_o = 1.5$

which combined with Eq. 1 yields

$$\bar{\epsilon} = \frac{2\bar{V}^3 f}{D_o} \tag{3}$$

An estimate of the Kolmogorov microscale is given by

$$\bar{\eta} = (\nu_c^3/\bar{\epsilon})^{1/4} \tag{4}$$

Using Eqs. 3 and 4 shows that for this study, the range $12{,}000 < Re < 21{,}000$ corresponds to $8.5 < \bar{\epsilon} < 50.5$ m^2/s^3 and $17.4 > \bar{\eta} > 11.5$ μm, respectively.

Initial and final Sauter mean diameters are given in Table 2. Typical initial and final drop size distributions are given in Figures 3 and 4. Complete distributions are given by Berkman (1985).

It is not our purpose to provide a detailed analysis of drop sizes produced by discharge of a capillary jet into a turbulent environment. However, some attention must be given to the initial size distribution to insure that the analysis of mixer performance is physically meaningful.

Table 2 shows that initial Sauter mean diameter D_{32} increases with increasing μ_d and decreasing Re. A comparison of the 50 mPa · s silicone oil and 45 mPa · s paraffin oil data indicates an increase in D_{32} with interfacial tension. The effect of μ_d and σ on final D_{32} is similar. However, final mean diameters decrease much more rapidly with Re. As a result, the ratio of initial to final D_{32} increases with Re and decreases with μ_d. This ratio varies from about 3 to 8 over the range of experiments. Any influence of initial drop size on mixer performance is best understood by examining drop size distribution.

Figure 3 shows that at low μ_d there is a finite but small overlap between initial and final drop size. The initial distributions are broader, with maximum overlap occurring at lower Re. However, only a small portion of the initial volume is affected; that is, less than 1% of the initial volume of dispersed phase entering the mixer is in drops that may not experience breakage. It is reasonable to assume that the final distribution, with the possible exception of the large size tail, is independent of conditions at the mixer entrance.

The situation becomes less satisfactory as μ_d increases, since initial distributions broaden rapidly and the degree of overlap increases. Figure 4 reveals that for the high-viscosity paraffin oil, the initial distribution is bimodal, containing many small

Table 2. Experimentally Determined Initial and Final Drop Diameters

Dispersed Phase	Nominal Dispersed Phase Visocisty μ_d' mPa · s	Reynolds Number 12,000 D_{32}, μm Init.	12,000 D_{32}, μm Final	15,000 D_{32}, μm Init.	15,000 D_{32}, μm Final	18,000 D_{32}, μm Init.	18,000 D_{32}, μm Final	21,000 D_{32}, μm Init.	21,000 D_{32}, μm Final
Silicone oil	20	1,890	483	1,431	309	1,380	245	1,098	183
	50	1,932	547	1,548	380	1,475	295	1,254	240
	100	2,355	704	1,877	468	1,718	355	1,510	300
	200	2,101	784	1,788	550	1,689	411	1,490	370
Paraffin oil	45	2,177	658	1,852	484	1,533	405	1,497	290
	150	2,716	920	2,422	614	2,328	509	1,951	393
p-Xylene	0.6	1,765	286	1,239	204	942	161	901	106

satellite droplets and a fairly narrow distribution of daughters (larger drops). At low *Re* as much as 5% of the initial drop volume may not experience breakage, thereby contributing to the large size tail of the final drop size distribution.

Despite these findings, it is reasonable to assume that drop sizes at the mixer exit are representative of mixer performance. It is possible that a drop slightly larger than D_{max}, entering this very long mixer, may not have sufficient time to break. However, such errors are tolerable given other errors inherent in the experimental procedure. Furthermore, the small volumes involved should not significantly affect the determination of final D_{32}. It is prudent, however, to consider the effect of initial drop size on the large size tail of the final size distribution, particularly at low *Re* and high μ_d.

Figure 5 shows the relationship between D_{32} and maximum stable drop size at the mixer exit. The data are well correlated by

$$D_{max} = 1.5 D_{32} \tag{5}$$

A similar result was found by Calabrese et al. (1986) and Wang and Calabrese (1986) in stirred tanks for the same physical property range. These authors argued mechanistically for such a relationship. The same arguments can be applied here.

Figures 3 and 4 show that the final drop size distribution exhibits almost straight-line behavior on normal probability coordinates and is therefore about normally distributed in volume. The distribution broadens with decreasing *Re* (or $\bar{\epsilon}$). Separate examination of the silicone oil and paraffin oil data shows that at constant *Re* and σ, the distribution broadens with increasing μ_d. The effects of dispersed phase viscosity and conditions of agitation on final drop size distribution are similar to those found by Calabrese et al. (1986) and Wang and Calabrese (1986) in stirred tanks.

Mean Drop Size Correlation

A mechanistic model for maximum stable drop size can be developed by equating the turbulent disruptive force acting upon the drop to the cohesive forces due to surface and internal viscous resistance to breakage. For $D = D_{max}$

$$\tau_c = C_1 \frac{\sigma}{D} + C_2 \frac{\mu_d}{D} (\tau_c/\rho_d)^{1/2} \tag{6}$$

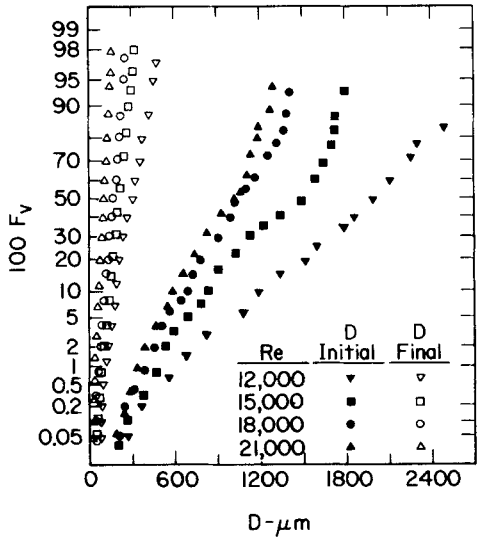

Figure 3. Drop size distribution at entrance and exit of mixer for *p*-xylene dispersed in water.
μ_d' = 0.6 mPa · s; σ = 31.8 mN · m^{-1}

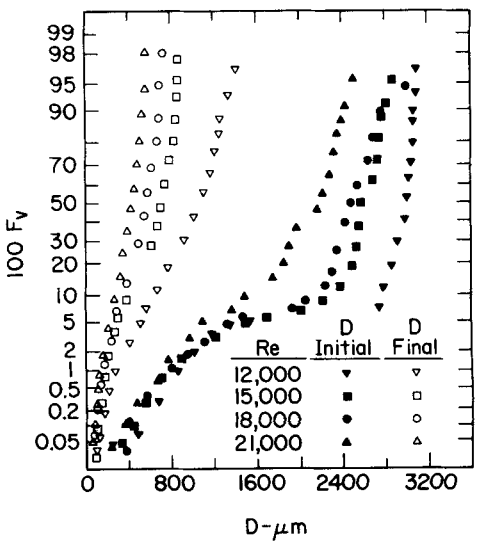

Figure 4. Drop size distributions at entrance and exit of mixer for the more viscous paraffin oil dispersed in water.
μ_d' = 150 mPa · s; σ = 41.6 mN · m^{-1}

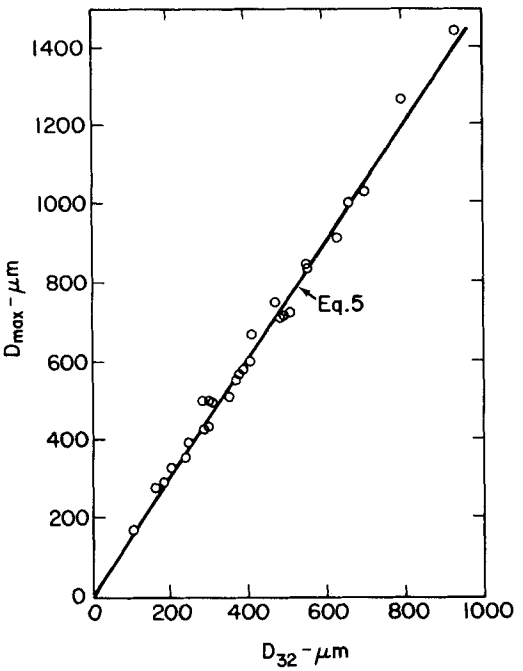

Figure 5. Relationship between maximum stable drop size and Sauter mean diameter at exit of mixer.

Equation 6 is consistent with arguments put forth by Kolmogorov (1949) and Hinze (1955). It is the same as that used by Hughmark (1971) to correlate the data of Sleicher (1962) and Paul and Sleicher (1965) for turbulent pipe flow and by Calabrese et al. (1986) to correlate their data for turbulent stirred tanks. Davies (1985, 1987) has argued that the form of Eq. 6 applies to a variety of turbulent emulsifiers.

In static mixers, the largest eddies are of order of 0.5 D_o while the smallest eddies are of order $\bar{\eta}$. The data of Figure 5 show that for the conditions of this study, maximum stable drop sizes are much larger than the microscale (reported earlier) but much smaller than the macroscale. These are the conditions for which Kolmogorov's theory for the inertial subrange applies, and τ_c is given by (Shinnar, 1961)

$$\tau_c = 1.5\alpha\rho_c\epsilon^{2/3}D^{2/3} \tag{7}$$

It is further assumed, following Chen and Middleman (1967) and Middleman (1974), that the local energy dissipation rate ϵ can be related to the mean energy dissipation rate $\bar{\epsilon}$ by a constant for geometrically similar systems. With $\epsilon = C_3\bar{\epsilon}$, Eqs. 5, 6, and 7 can be combined to yield

$$D_{32} = C_4\left(\frac{\sigma}{\rho_c\bar{\epsilon}^{2/3}}\right)^{3/5}\left[1 + C_5\frac{\mu_d\bar{\epsilon}^{1/3}D_{32}^{1/3}}{\sigma}\left(\frac{\rho_c}{\rho_d}\right)^{1/2}\right]^{3/5} \tag{8}$$

For dilute suspensions, Eq. 8 can be combined with Eq. 3 to yield

$$\frac{D_{32}}{D_o} = C_6We^{-3/5}f^{-2/5}\left[1 + C_7f^{1/3}Vi\left(\frac{D_{32}}{D_o}\right)^{1/3}\right]^{3/5} \tag{9}$$

where $V_i = (\mu_d\bar{V}/\sigma)(\rho_c/\rho_d)^{1/2}$ is a viscosity group or capillary number representing the ratio of viscous to surface forces acting to stabilize the drop. Sleicher (1962) correlated his pipe flow data by arguing for such a viscosity group on physical grounds.

For the static mixer of this study f is constant for $Re >$ 12,000. Therefore, for the data reported here, Eq. 9 reduces to

$$\frac{D_{32}}{D_o} = AWe^{-3/5}\left[1 + BVi\left(\frac{D_{32}}{D_o}\right)^{1/3}\right]^{3/5} \tag{10}$$

Equation 10 is of exactly the same form as the correlation developed by Wang and Calabrese (1986) for stirred tanks. The empirical constants A and B will differ due to geometric factors contained in the definitions of We and Vi, differences in the spatial distribution of energy dissipation rate, and possibly to differences in the breakage mechanism. Equation 10 reduces to Eq. 1 in the limit of negligible viscous resistance to breakage ($Vi \rightarrow 0$).

The constants A and B can be obtained by linear least-squares regression from a plot of $We(D_{32}/D_o)^{5/3}$ vs. $Vi(D_{32}/D_o)^{1/3}$. The result with all data points weighted equally is

$$\frac{D_{32}}{D_o} = 0.49We^{-3/5}\left[1 + 1.38Vi\left(\frac{D_{32}}{D_o}\right)^{1/3}\right]^{3/5} \tag{11}$$

The goodness of fit of Eq. 11 is shown in Figure 6. The correlation coefficient is 0.85. It should be noted that linear plots of this type tend to emphasize scatter in the data relative to the more commonly employed log-log plots such as Figure 7. It is seen that Eq. 11 provides a good fit to the data although some dependency on Re is apparent. There are several plausible explanations for the scatter in the data. Although unlikely, the mixer may not be long enough to insure an equilibrium suspension at its exit. There may be some residual effect of initial drop size, particularly at low Re and high μ_d. Some Reynolds numbers may not be high enough to insure an inertial subrange. The steep mean velocity gradients close to the mixer surfaces or the coherent wake structures behind the individual elements may play some role in droplet dispersion. Such secondary hydrodynamic effects would cast suspicion on the use of Eq. 7.

In the inviscid limit ($Vi \rightarrow 0$), Eq. 11 reduces to

$$\frac{D_{32}}{D_o} = 0.49We^{-3/5} \tag{12}$$

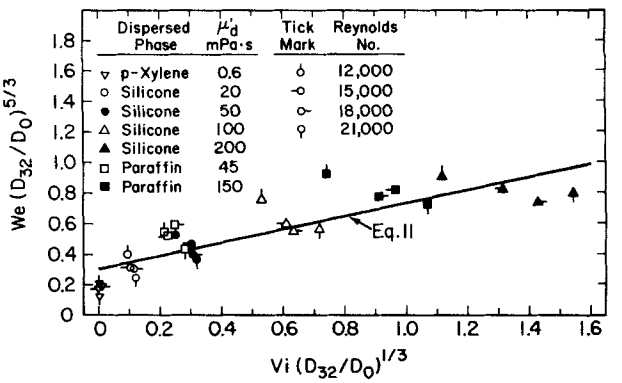

Figure 6. Correlation for equilibrium mean drop size.

Figure 6 shows that Eq. 11 tends to overpredict the *p*-xylene ($\mu_d' = 0.6$ mPa · s) data, so it is prudent to assess the applicability of Eq. 12 to surface force stabilized dispersions. Middleman (1974) obtained substantial data for dilute suspensions of low-viscosity ($\mu_d \leq 1$ mPa · s) organics in water in two 21-element Kenics mixers of the pitch employed here. These and the *p*-xylene data of this study are given in the Weber number plot of Figure 7. Equation 12 is seen to provide a good fit, indicating that the data of this study are consistent with the equilibrium inviscid dispersed phase data of Middleman and that in the inviscid limit, Eq. 11 applies to a broader range of system variables than employed here.

While Middleman considered the Reynolds number range of this study, most of his data were acquired at lower *Re* where the friction factor depends weakly upon *Re*, Figure 2. Therefore, Eq. 12 is not strictly valid and the inviscid limit of Eq. 9 should be used to correlate his data. This approach did not yield an improved fit. This is consistent with Middleman's argument that the dependency of f on *Re* is too weak to warrant consideration.

Middleman also reported data for two slightly viscous organics dispersed in water. These could not be correlated by Eq. 11. In Figure 6 the ordinate was up to 5 and 12 times larger than that of Eq. 11 for his benzyl alcohol (5 mPa · s) and oleic acid (26 mPa · s) data, respectively. The reason for this is not apparent; it could not be attributed to lower Reynolds number. Middleman reported that models containing a viscosity group as a second parameter failed with these data.

It should be noted that Middleman maintained holdup below 1% by volume. On the average his volume fractions, although dilute, were an order of magnitude greater than those employed here. Viscous drops are more likely to coalesce. His conclusion that the effect of ϕ on D_{32} is negligible was based on $\mu_d = 0.6$ mPa · s and $\phi \geq 0.01$. Figure 7 shows that Middleman's low-viscosity data lie slightly above ours. It may be that some role is played by coalescence in the range $0.001 < \Phi < 0.01$ and that it becomes more pronounced as μ_d increases. A final consideration is that the oleic acid-water system exhibits complex interfacial phenomena whose role in liquid-liquid dispersion is difficult to quantify.

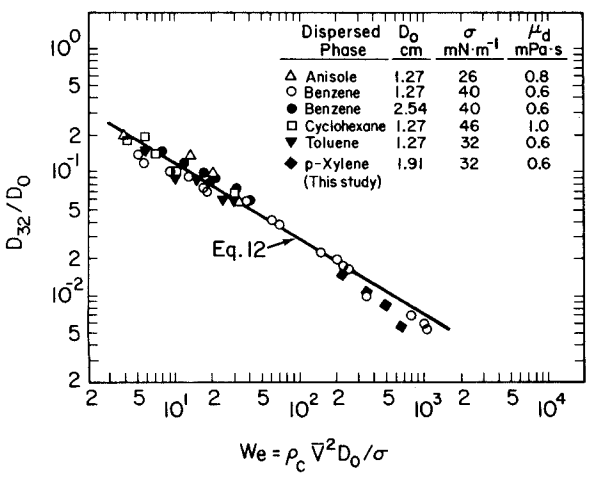

Figure 7. Comparison of Eq. 12 with data for inviscid dispersed phases.
For all data the continuous phase is water
Except for *p*-xylene all data are those of Middleman (1974)

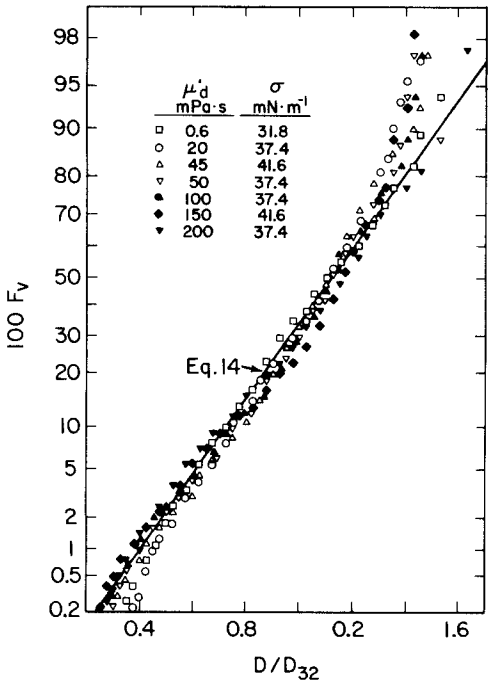

Figure 8. Similarity of normalized volume distribution at mixer exit for constant conditions of agitation.
Re = 18,000

Correlation for Final Drop Size Distribution

Consider a relative resistance to breakage defined as the ratio of cohesive to disruptive forces acting upon a drop. If these forces are described as in Eq. 6 with τ_c given by Eq. 7 with 3, one finds that for a given drop size, the relative resistance to breakage increases with μ_d and σ and decreases with *Re* or $\bar{\epsilon}$. As previously discussed, the broadness of the final drop size distribution follows the same trends so that this relative resistance becomes a measure of said. Therefore, it can be assumed that the probability density function which describes the distribution should depend only upon the relative resistance to breakage. Wang and Calabrese (1986) used exactly these arguments to show that, to a first approximation, the equilibrium drop size distribution produced in stirred tanks can be correlated by normalization with D_{32}. The argument for static mixers is the same and will not be repeated here. Instead we will simply seek a correlation of the form $F_v(D/D_{32})$.

Normalized drop size distributions for the seven different dispersed phases are given at *Re* = 18,000 in Figure 8. Berkman (1985) provides the complete set. The distributions are not quite normally distributed in volume, displaying a slight sinusoidal variation. Middleman's (1974) data were similar. Except for scatter in the tails, normalization with D_{32} appears to provide an adequate correlation. Since the distributions are about normally distributed in volume, the normalized frequency can be approximated by (Wang and Calabrese, 1986):

$$F_v(X) = 0.5\left[1 + \text{erf}\left(\frac{X - \bar{X}}{\sqrt{2}\sigma_v}\right)\right] \tag{13}$$

where $X = D/D_{32}$ and $\bar{X}$ and σ_v are the volume-weighted mean and standard deviation, respectively.

The data were fitted to Eq. 13 by nonlinear least-squares regression. On the average, 43 points in the range $0.002 < F_v < 0.99$ were used to describe each distribution. The result was

$$F_v(D/D_{32}) = 0.5\left[1 + \text{erf}\left(\frac{D/D_{32} - 1.12}{0.31\sqrt{2}}\right)\right] \qquad (14)$$

The root mean square deviation, based on the difference between the experimental and predicted values of F_v normalized by the former, was 26%. The goodness of fit of Eq. 14 is visualized in Figure 8. The greatest deviations appear in the large size tail. The data of Figures 3 and 4 indicate that this may be a residual effect of the size distribution at the mixer entrance. If these deviations are solely due to initial drop size, then from the previous discussion one would expect the degree of scatter to increase with increasing μ_d and decreasing Re. No such correlation was found. It is more likely that these deviations are inherent in the experimental technique. It is not reasonable to expect an accurate representation of the large size tail of the third moment (volume) of the measured variable (diameter) from a sample population of 300 counts.

Middleman (1974) found that his equilibrium data were well correlated by Eq. 13 with $\overline{X} = 1.06$ and $\sigma_v = 0.25$. The data of this study show a slightly higher mean and a larger standard deviation. The increased broadness may be due to the higher dispersed phase viscosities employed here or may indeed be a residual effect of initial drop size. The latter is difficult to assess since Middleman did not provide information on his initial drop size. He also introduced the dispersed phase through a capillary tube. For stirred vessels, Wang and Calabrese (1986) reported that their correlation for cumulative volume frequency for a similar range of viscous dispersed phases was exactly the same as that of Chen and Middleman (1967) for inviscid drops. However, this conclusion was based upon a comparison of at least five times as much data as employed here.

Discussion

Equations 8 and 10 are equally valid forms of the mean size correlation. The later may appear more desirable since it contains only system variables. However, the form of Eq. 8 should be used to compare different devices since, for constant physical properties, it allows determination of dispersion efficiency at equal energy input. Using Eq. 3 with $f = 0.416$ and the definitions of We and Vi, it can be shown that Eq. 11 is equivalent to Eq. 8 with $C_4 = 0.416$ and $C_5 = 1.47$.

The correlation of Wang and Calabrese (1986) for stirred tanks equipped with Rushton turbines of half the tank diameter can also be recast in the form of Eq. 8. The result (power no. = 6) is $C_4 = 0.054$ and $C_5 = 4.11$. While the dependency on μ_d is greater, the stirred tank produces much smaller drops than the Kenics mixer. A comparison of Eq. 14 with Eq. 23 of Wang and Calabrese shows that tank drop size distributions are also narrower. These results are not surprising since the ratio of local to mean energy dissipation rate is large in the impeller region while dissipation rate is more uniformly distributed in the static mixer. A more reasonable comparison should also account for the time/distance to reach equilibrium.

Recently, Davies (1987) has shown that it is possible to develop an approximate device independent correlation for D_{max} in terms of the maxima in ϵ. This approach should only be used in the absence of specific correlations since the spatial variation of ϵ can only be approximated for most turbulent contactors and it has not been established that breakage mechanism is device-independent.

Acknowledgment

This work was partially supported by grants from the Minta Martin Fund for Aeronautical Research (University of Maryland) and the Center for Chemical Engineering, National Bureau of Standards (No. 7ONANH0021). The authors wish to thank Carl Stoots, who measured the friction factor data, and David Dickey, formerly of Chemineer-Kenics Inc., who provided the static mixer.

Notation

A, B = dimensionless empirical constants
$C_1, \ldots, C_7$ = dimensionless empirical constants
D = drop size
D_{max} = maximum stable drop size
D_o = pipe on static mixer diameter
D_{32} = Sauter mean diameter
F_v = cumulative volume frequency
f = Fanning friction factor
L = length of mixer
L_e = length of single mixer element
n_e = number of mixer elements
ΔP = pressure drop across mixer
$Re = \overline{V}D_o/\nu_c$, Reynolds number
$\overline{V}$ = mean velocity of continuous phase in mixer based on cross section of empty pipe
$Vi = (\mu_d\overline{V}/\sigma)(\rho_c/\rho_d)^{1/2}$, viscosity group on capillary number
$We = \rho_c\overline{V}^2/\sigma$, Weber number
$X = D/D_{32}$, normalized drop diameter
$\overline{X}$ = volume-weighted mean of X

Greek letters

α = Kolmogorov constant
ϵ = local energy dissipation rate per unit mass
$\bar{\epsilon}$ = mean energy dissipation rate per unit mass
$\overline{\eta}$ = Kolmogorov microscale based on mean energy dissipation rate
μ_d = viscosity of dispersed phase
μ_d' = nominal dispersed phase viscosity
ν_c = kinematic viscosity of continuous phase
ρ_c = density of continuous phase
ρ_d = density of dispersed phase
σ = interfacial tension
σ_v = volume-weighted standard deviation of X
τ_c = turbulent disruptive force per unit area acting on drop
Φ = holdup or volume fraction of dispersed phase

Literature Cited

Al Taweel, A. M., and L. D. Walker, "Liquid Dispersion in Static In-Line Mixers," *Can. J. Chem. Eng.*, **61**, 527 (1983).

Berkman, P. D., "Drop Size Distributions Produced in a Static Mixer," M.S. Thesis, Univ. Maryland, College Park, MD (June, 1985).

Bird, R. B., W. E. Stewart, and E. N. Lightfoot, *Transport Phenomena*, Wiley, New York (1960).

Calabrese, R. V., T. P. K. Chang, and P. T. Dang, "Drop Breakup in Turbulent Stirred-Tank Contactors. I: Effect of Dispersed Phase Viscosity," *AIChE J.*, **32**, 657 (1986).

Chen, S. J., and D. R. Libby, "Gas-Liquid and Liquid-Liquid Dispersion in a Kenics Mixer," *AIChE 71st Ann. Meet.*, Miami (Nov., 1978).

Chen, H. T., and S. Middleman, "Drop Size Distribution in Agitated Liquid-Liquid Systems," *AIChE J.*, **13**, 989 (1967).

Davies, J. T., "Drop Sizes of Emulsions Related to Turbulent Energy Dissipation Rates," *Chem. Eng. Sci.*, **40**, 839 (1985).

———, "A Physical Interpretation of Drop Sizes in Homogenizers and

Agitated Tanks, Including the Dispersion of Viscous Oils," *Chem. Eng. Sci.*, **42**, 1671 (1987).
Haas, P. A., "The Dispersion of Aqueous Drops in Organic Liquids," *AIChE J.*, **33**, 987 (1987).
Hinze, J. O., "Fundamentals of the Hydrodynamic Mechanism of Splitting in Dispersion Processes," *AIChE J.*, **1**, 289 (1955).
Hughmark, G. A., "Drop Breakup in Turbulent Pipe Flow," *AIChE J.*, **17**, 1000 (1971).
Kolmogorov, A. N., "The Breakup of Droplets in a Turbulent Stream," *Dok. Akad. Nauk.*, **66**, 825 (1949).
Middleman, S., "Drop Size Distributions Produced by Turbulent Pipe Flow of Immiscible Fluids through a Static Mixer," *Ind. Eng. Chem. Process Des. Dev.*, **13**, 78 (1974).
Paul, H. I., and C. A. Sleicher, Jr., "The Maximum Stable Drop Size in Turbulent Flow: Effect of Pipe Diameter," *Chem. Eng. Sci.*, **20**, 57 (1965).
Shinnar, R., "On the Behavior of Liquid Dispersions in Mixing Vessels," *J. Fluid Mech.*, **10**, 259 (1961).
Sleicher, C. A., Jr., "Maximum Stable Drop Size in Turbulent Flow," *AIChE J.*, **8**, 471 (1962).
Tavlarides, L. L., and M. Stamatoudis, "The Analysis of Interphase Reactions and Mass Transfer in Liquid-Liquid Dispersions," *Adv. Chem. Eng.*, **11**, 199 (1981).
Wang, C. Y., and R. V. Calabrese, "Drop Breakup in Turbulent Stirred-Tank Contactors. II: Relative Influence of Viscosity and Interfacial Tension," *AIChE J.*, **32**, 667 (1986).

Manuscript received July 22, 1986, and revision received Dec. 9, 1987.